

Neuron, Volume 112

## Supplemental information

### Monitoring norepinephrine release *in vivo* using next-generation GRAB<sub>NE</sub> sensors

Jiesi Feng, Hui Dong, Julieta E. Lischinsky, Jingheng Zhou, Fei Deng, Chaowei Zhuang, Xiaolei Miao, Huan Wang, Guochuan Li, Ruyi Cai, Hao Xie, Guohong Cui, Dayu Lin, and Yulong Li

**Inventory of Supplemental Information:**

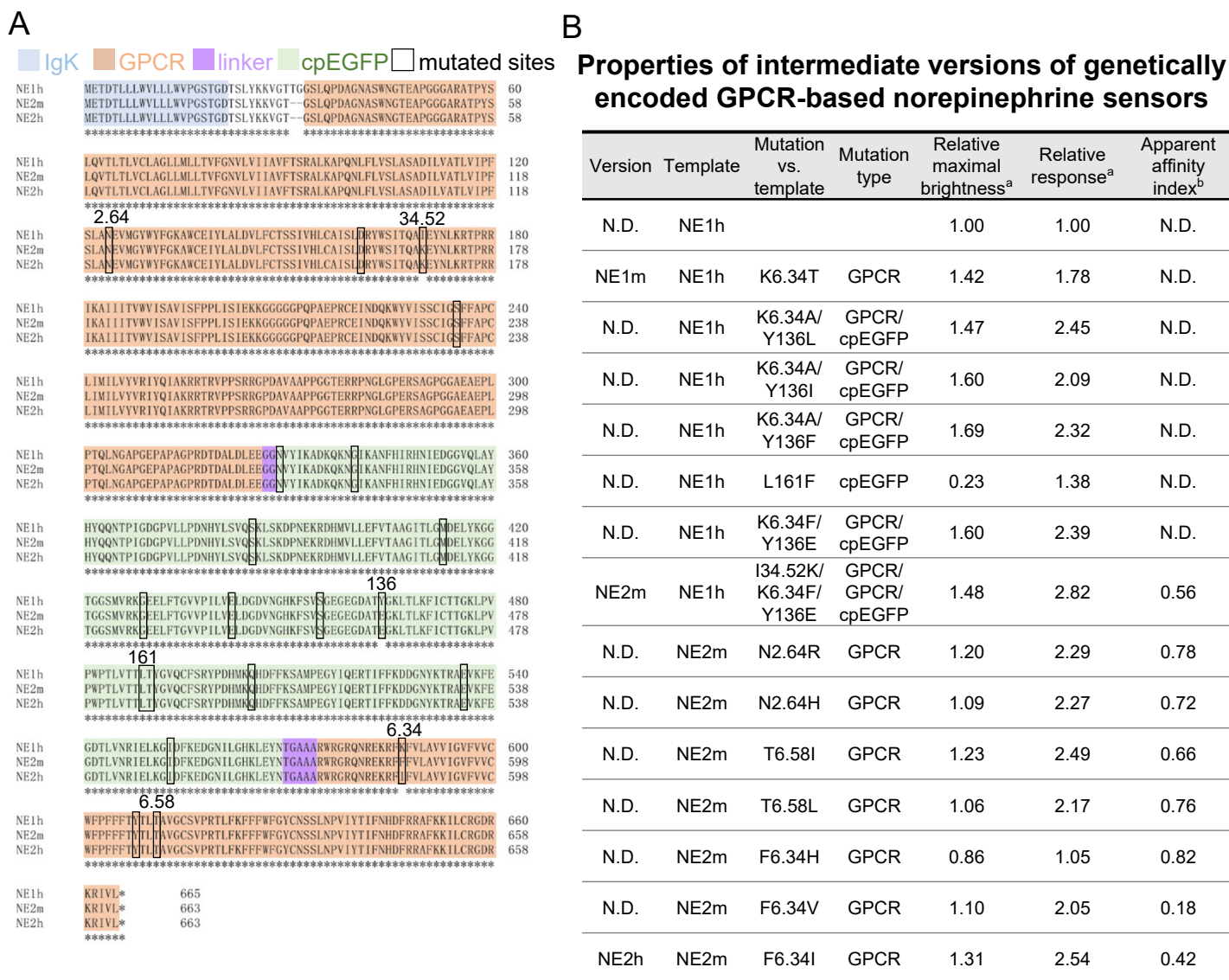
**Figure S1.** Amino acid sequence alignments and properties of GRAB<sub>NE</sub> versions and intermediates, related to Figure 1.

**Figure S2.** Characterization of next-generation GRAB<sub>NE</sub> sensors in cultured HEK293T cells or neurons, related to Figure 1.

**Figure S3.** Characterization of next-generation GRAB<sub>NE</sub> sensors *in vivo*, related to Figure 4.

**Figure S4.** GRAB<sub>NE2m</sub> and GRAB<sub>NEmut</sub> fluorescence measured during audio stimulation, related to Figure 5.

**Figure S5.** Mesoscopic NE and calcium dynamics in dorsal cortex of awake mice, related to Figure 5.



<sup>a</sup> Relative data were determined by maximal brightness or response to NE1h; <sup>b</sup> apparent affinity index were determined by response in 10 μM divide response in 300 nM NE; N.D.: not determined;

**Note:** All data were collected in HEK293T cells.

**Figure S1. Amino acid sequence alignments and properties of GRAB<sub>NE</sub> versions and intermediates, related to Figure 1.**

(A) Sequence alignments of GRAB<sub>NE1h</sub>, GRAB<sub>NE2m</sub>, and GRAB<sub>NE2h</sub>. The selected mutation sites were indicated by the black box.

(B) Properties of intermediate versions of genetically encoded GPCR-based norepinephrine sensors. The beneficial mutation sites and intermediates were summarized with brightness, response and apparent affinity index.

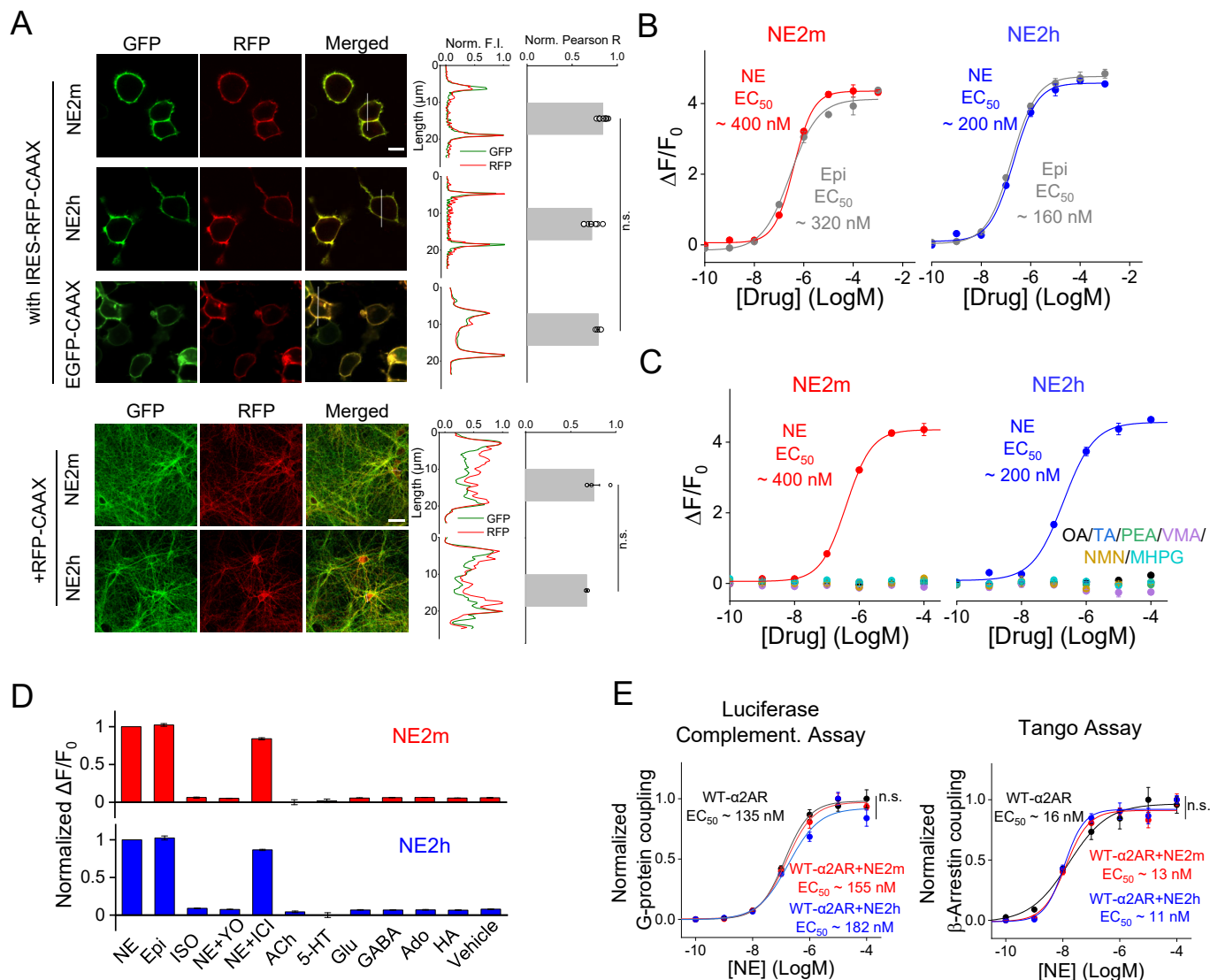


**Figure S2. Characterization of next-generation GRAB<sub>NE</sub> sensors in cultured HEK293T cells or neurons, related to Figure 1.**

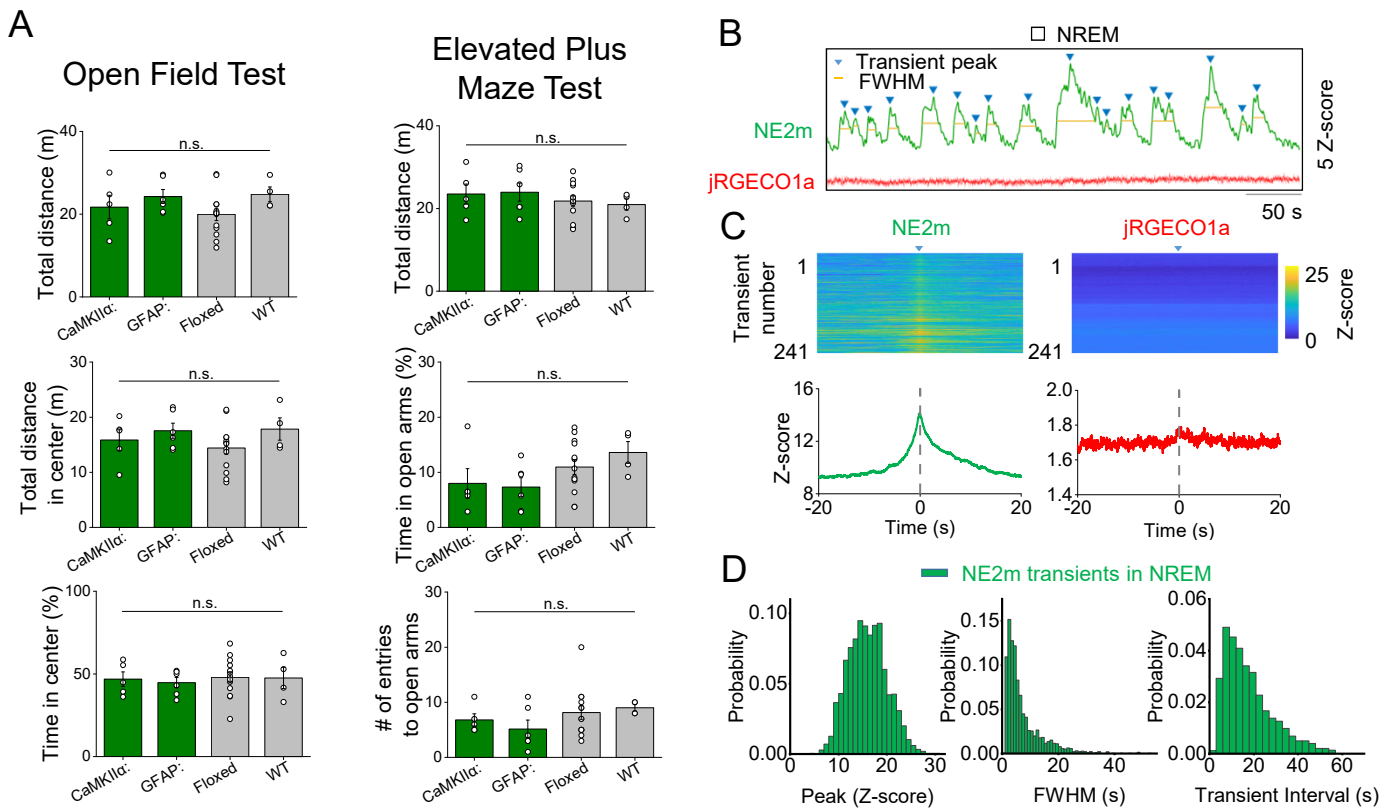
Expression of GRAB<sub>NE</sub> sensors, membrane-localized EGFP and RFP in cultured HEK293T cells (top) and neurons (bottom). Line plotting of GFP and RFP signals were shown in middle. Normalized colocalization ratio with membrane-target RFP were summarized in right. The scale bar is 10  $\mu\text{m}$  (top) and 50  $\mu\text{m}$  (bottom). Dose-dependent curves of GRAB<sub>NE2m</sub> and GRAB<sub>NE2h</sub> in response to a variety concentrations of norepinephrine (NE) and epinephrine (Epi) in HEK293T cells. The corresponding  $EC_{50}$  values are indicated.  $n = 3$  independent cultures each.

(C) Dose-dependent response of GRAB<sub>NE2m</sub> and GRAB<sub>NE2h</sub> to trace amines (OA: octopamine, TA: tyramine, PEA: phenethylamine) and major NE metabolites (VMA: vanillylmandelic acid, NMN: normetanephrine, MHPG: 3-methoxy-4-hydroxyphenylglycol) in HEK293T cells.  $n = 3$  independent cultures each.

(D) Normalized changes in the fluorescence intensity of GRAB<sub>NE2m</sub> (top) and GRAB<sub>NE2h</sub> (bottom) in response to application of the indicated molecules (applied at 10  $\mu\text{M}$ ),  $\Delta F/F_0$  relative to NE. NE, norepinephrine; Epi, epinephrine; ISO, isoprenaline; YO, yohimbine; ICI, ICI-118,551; ACh, acetylcholine; 5-HT, 5-hydroxytryptamine (serotonin); Glu, glutamate; GABA,  $\gamma$ -aminobutyric acid; Ado, adenosine; HA, histamine.

(E) Downstream G protein signaling (left) and  $\beta$ -arrestin signaling (right) of the native wildtype  $\alpha 2$  adrenergic receptor (WT- $\alpha 2\text{AR}$ ) with or without co-expression of GRAB<sub>NE</sub> sensors measured using a luciferase complementation mini-G protein assay and the Tango assay in cultured cells, respectively.  $n = 3$  wells with  $\geq 10^5$  cells.

n.s., not significant (one-way ANOVA for A and two-way ANOVA for E).



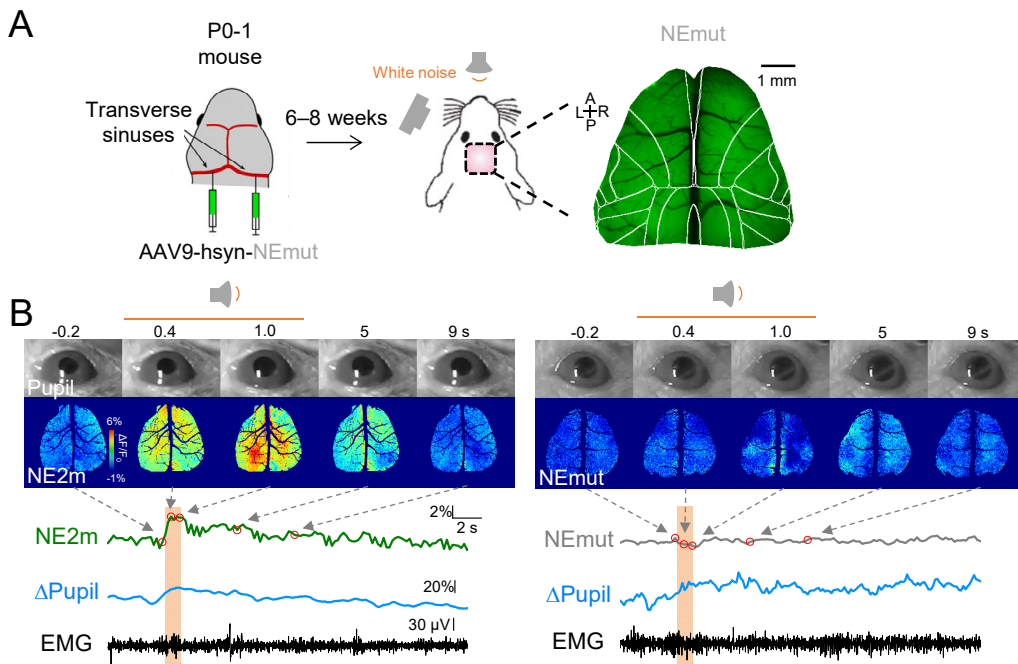


**Figure S4. GRAB<sub>NE2m</sub> and GRAB<sub>NEmut</sub> fluorescence measured during audio stimulation, related to Figure 5.**

(A) Schematic diagram depicting the delivery of AAV in P0–P1 mouse pups by injection into the transverse sinuses in P0–P1 mouse for expressing GRAB<sub>NEmut</sub> in neurons in the dorsal cortex. Also shown are an image of GRAB<sub>NEmut</sub> fluorescence and the paradigm used for audio stimulation using white noise.

(B) Representative images and time course of the change in diameter pupil, GRAB<sub>NE2m</sub> (left) and GRAB<sub>NEmut</sub> (right) fluorescence measured in the cortex, and the EMG recording. The shaded areas indicate the delivery of white noise.

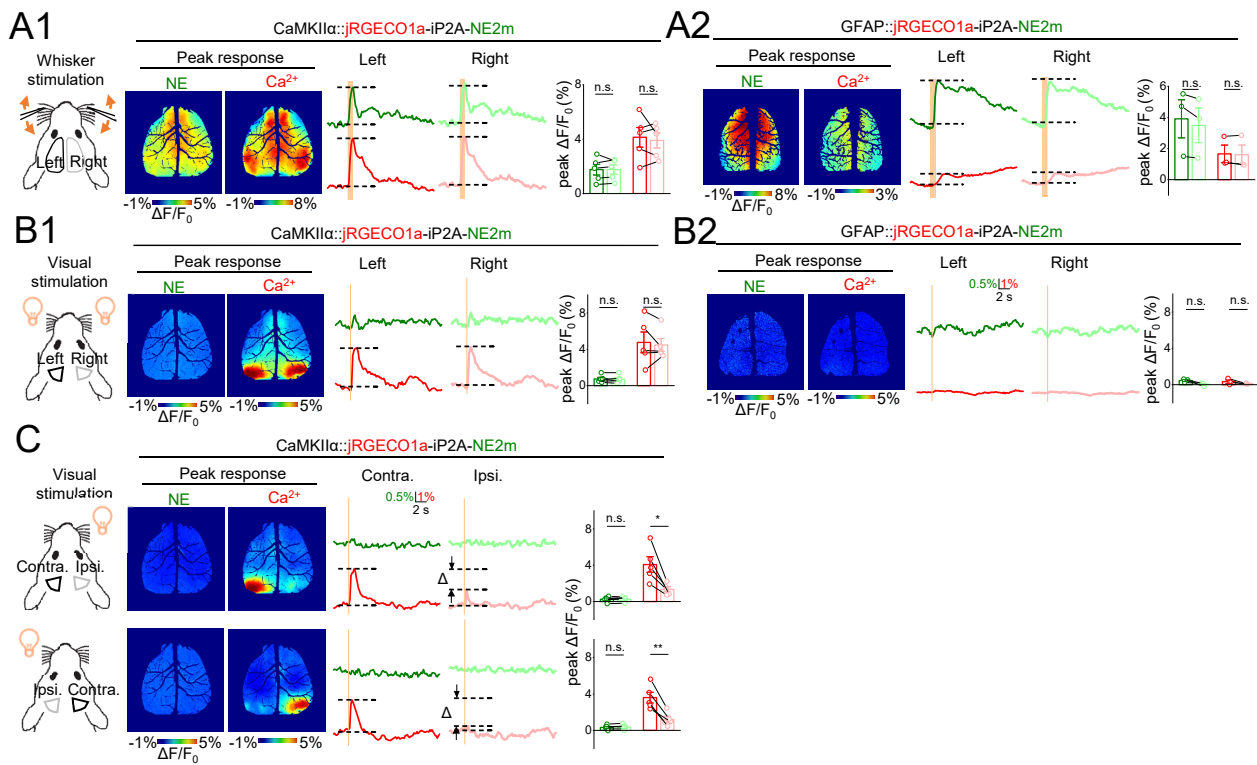


**Figure S5. Mesoscopic NE and calcium dynamics in dorsal cortex of awake mice, related to Figure 5.** (A–C) Illustrations (left) of whisker stimulation and visual stimulation delivered to CaMKII $\alpha$ ::NECa and GFAP::NECa mice. Shown are the peak response images, representative traces, and summary of the peak responses following bilateral (A–B) or unilateral (C) stimulation of the indicated mice. black and grey lines indicate the ROIs used to analyze the representative traces.  $n = 3\text{--}5$  animals per group. \*\* $p < 0.01$ , \* $p < 0.05$ , and n.s., not significant (Paired student's  $t$ -test).